Russian Chemical Reviews

January 1987

Translated from *Uspekhi Khimii*, **56**, 3-28 (1987)

U.D.C. 541.1:548.55:546.271'654

Physicochemical Problems in the Preparation of Defect-free Monocrystals of Lanthanum Hexaboride

M.M.Korsukova and V.N.Gurin

The physicochemical basis of the preparation of single crystals of stoichiometric lanthanum hexaboride (a promising new material for emission electronics) is discussed. It is shown that stoichiometric defect-free monocrystals can be prepared only by allowing for the form of the homogeneity region in the phase diagram of the crystalline compound. Studies of defects in the crystal structure are reviewed, and their results are shown to be related to the form of the homogeneity of lanthanum hexaboride. Some physicochemical properties and some possible applications of lanthanum hexaboride monocrystals are examined.
The bibliography includes 150 references.

CONTENTS

I. Introduction
II. Homogeneity region of lanthanum hexaboride and preparation of monocrystals of stoichiometric composition
III. Methods of preparing lanthanum hexaboride monocrystals
IV. Some properties of lanthanum hexaboride monocrystals

I. INTRODUCTION

Lanthanum hexaboride is used in several new instruments (electron microscopes, microanalysers, Auger spectrometers) to study the surface and other properties of materials of various types. However, the preparation of perfect and very pure single crystals of lanthanum hexaboride for use in the cathodes of these instruments still presents some unsolved problems. This is because of the difficulty in controlling the chemical composition and in achieving a high level of structural perfection, and also in establishing adequate quality control.

Many papers have been published on lanthanum hexaboride, dealing mainly with the preparation of LaB_6 monocrystals, with studies of their composition, structure, and properties, and with their emission properties and practical applications. We have recently published a comprehensive review[1] of work on the preparation of LaB_6 monocrystals and on their properties and potential applications, but little emphasis was placed on the physicochemical conditions needed to prepare very perfect LaB_6 monocrystals.

The aim of the present review is to highlight the physicochemical problems underlying the preparation of stoichiometric and defect-free monocrystals of LaB_6.

II. HOMOGENEITY REGION OF LANTHANUM HEXABORIDE AND PREPARATION OF MONOCRYSTALS OF STOICHIOMETRIC COMPOSITION

Though lanthanum hexaboride has been known for a long time,[2] we have little reliable information on the phase diagram of the La–B system and especially on the homogeneity region

of LaB_6. The phase diagram of the La–B system was first described by Johnson and Daane,[3] and a modified diagram was subsequently published to include new data.[4] In the most recent publications[5,6] the part of the phase diagram of the La–B system containing the compound LaB_6 is examined. At present two compounds have been reliably identified in the La–B system: 1) LaB_4, which melts incongruently at 2073 K with formation of LaB_6 and of a liquid phase containing 66.7 at.% of B,[3] and 2) LaB_6, which melts congruently at 2988 K.[4,5]

The compound LaB_4 has a tetragonal crystal lattice (UB_4 structure type) with lattice constants $a = 7.324 \pm 0.001$ Å and $c = 4.181 \pm 0.001$ Å;[7] its homogeneity region is very narrow.

The compound LaB_6 has a cubic lattice (CaB_6 structure type).[8] Its crystal structure can be treated as body-centred cubic, with La atoms and octahedra of B atoms occupying positions analogous to those of the Cs^+ and Cl^- ions in the CsCl structure.[9] Each lanthanum atom is surrounded by 24 boron atoms, and each boron atom forms five B–B bonds: four with boron atoms in the same octahedron and the fifth with a boron atom from a neighbouring octahedron.

Published information on the homogeneity region of LaB_6 is inconsistent, and describes the region as broad[3,10] or as relatively narrow.[5,6,11–16] However, in either case the defect structure of the LaB_6 crystal is attributed to defects in the metal (La) sublattice (assumed to be few in the case of a narrow region). The lattice constant of the LaB_6 crystal is found (experimentally) to be unaffected by the defect density.[5,11,17,18] Lastly, some workers have detected a LaB_9 phase with the same structure, and lattice constant, as the LaB_6 phase.[5,19]

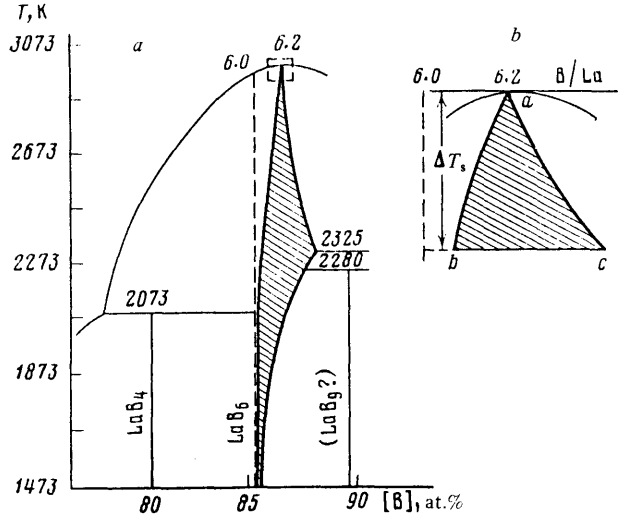


Figure 1. Part of the La–B phase diagram:[5] *a*) is the homogeneity region of LaB_6 *b*) is an enlarged presentation of the high-temperature part of LaB_6 homogeneity region, showing the supercooling ΔT_S.

Existing data on the La–B system suggest a number of conclusions of direct relevance to the preparation of stoichiometric single crystals of LaB_6. Fig.1 shows a part of the phase diagram of the La–B system including the existence region of lanthanum hexaboride.[5] We note that the homogeneity region of LaB_6, which begins at ~2073 K, broadens rapidly as far as 2325 K (the temperature of the LaB_6–B eutectic) and remains fairly wide up to T_m (the melting point of LaB_6) (the "upper" part of the homogeneity region has been described[6] as "narrow" because it is slightly shifted from the stoichiometric composition B/La = 6, and the same description is used in Ref.5). The deviation of the singularity for lanthanum hexaboride from the stoichiometric proportion B/La = 6 is, in fact, substantial: approximately 0.2 atom fraction of B, i.e. to $LaB_{6.2}$. The homogeneity region of the hexaboride is widest (from $LaB_{6.1}$ to $LaB_{6.7}$) at $T_{eut} = 2325$ K. Inspection of this region near the singularity, i.e. at T_m of lanthanum hexaboride (see Fig.1*b*), leads to important conclusions regarding the actual composition of the monocrystals obtained from melts at these temperatures (for example, by zone melting).

Thus, if the supercooling of a melt of stoichiometric composition in the crystallisation volume reaches the value ΔT_S the composition of the resulting hexaboride monocrystals is described by the point *b* (for example, $LaB_{6.1}$). Since ΔT_S can vary from a fraction of a degree to hundreds of degrees, and is not easy to control, especially at high temperatures, the composition of the grown crystals can also be uncontrolled. If the composition of the melt at the beginning of the crystallisation corresponds to the point *a* (i.e. to $LaB_{6.2}$) the resulting monocrystals will also have this composition. On the other hand if the initial composition deviates on either side of the point *a* the composition of the resulting crystals will correspond to points on the *ab* or *ac* boundaries of the homogeneity region. This provides our first important conclusion: if the published data[5] for the La–B phase diagram are correct, the preparation of lanthanum hexaboride monocrystals of stoichiometric composition by a liquid-phase method, i.e. from the corresponding melt, is impossible.

Another important aspect of this problem is that the compound LaB_6 dissociates fairly strongly at $T = T_m$. Hence in order to prepare monocrystals from the melt we need to apply an overpressure of a few tens of atmospheres. We also know that at T_m of lanthanum hexaboride the La partial vapour pressure is much higher than the pressure of B.[20] Therefore in order to prepare a melt of the required initial composition (for example, $LaB_{6.2}$) we must introduce the correct B/La component ratio into the initial charge. This means that LaB_6 monocrystals prepared from the stoichiometric melt will always contain an excess of B and consist of a two-phase system or of a solid solution of B in LaB_6. These solid solutions can decompose into LaB_6 and B at low temperatures due to the narrowing of the homogeneity region. This assumption is confirmed to some extent by the presence of B inclusions in LaB_6 monocrystals.[21]

The strong narrowing of the LaB_6 homogeneity region below 2280 K, accompanied by a shift of the left-hand boundary which brings it almost exactly to the stoichiometric LaB_6 composition at 1673–1773 K, suggests another conclusion: LaB_6 monocrystals of stoichiometric composition can be prepared only by methods which are applicable at temperatures not higher than 1673 K.

III. METHODS OF PREPARING LANTHANUM HEXABORIDE CRYSTALS

Only three of the four methods of preparing monocrystals of refractory compounds (according to our classification[22]) have so far been applied to the growth of LaB_6 monocrystals: gas-phase, liquid-phase, and solution methods. We shall consider the special features of each of these methods separately, and compare their technological advantages and their potential suitabilities for the production of stoichiometric monocrystals.

1. The Gas-Phase Method

This method consists in the transport of the substance to be crystallised through the gas phase to the substrate by generating a temperature or concentration gradient between the source and the substrate or by chemical gas-transport reactions. Depending on the chosen method of transport, the monocrystals are grown in a vacuum or in the presence of a carrier. Halogens or halogen–hydrogen mixtures are often used in the preparation of LaB_6 (see Table 1). In any particular method the following crystal growing procedures can be used: a) sublimation, or ΔT transport (when the substance to be crystallised has a high vapour pressure and a congruent evaporation); b) chemical, or Δc transport (when the vapour pressure is low); c) transport of the substance to be crystallised in an electric arc (for a low vapour pressure and a high melting point); d) chemical reaction in the gas phase (in which the synthesis precedes the crystallisation of the substance). Only Δc transport[23,24] and chemical reactions[25,26] have been used so far, from the above list, to prepare LaB_6 monocrystals:

$$La_2O_3 + H_2 + BCl_3 \rightarrow LaB_6 + HCl$$

$$LaCl_3(g) + 6BCl_3(g) + (21/2)H_2(g) \rightarrow LaB_6(s) + 21HCl$$

Table 1. Preparation of LaB_6 monocrystals by the gas-phase method.

Method of preparation	Preparative conditions			Characteristics of the resulting crystals		Refs.
	T, K	time, h	other conditions	shape and size, mm	other characteristics	
Δc transport Br_2 carrier	1423–1173	–	initial charge LaB_6 powder, Ar inert gas	needles; 0.50 × 0.15 × 2.00	colour violet	[23]
Δc transport carriers (H_2 + BBr_3) or (H_2 + Br_2)	1273–1573	–	initial charge LaB_6, substrate sintered LaB_6	⟨100⟩ whiskers, pyramidal crystals	–	[24]
Chemical reactions	zone *A* 1273; zone *B* 1623–1723	3	initial charge pressed La_2O_3; substrate graphite	{100} cubes, {111} cubo-octahedra; 1 × 1 × 1	colour purple	[25]
Chemical reactions	1373–1623	0.5–2	substrate graphite, $BCl_3/LaCl_3$ = 10:1, atmospheric pressure	⟨100⟩ whiskers; l = 2–5, thickness 0.001–0.020; ⟨100⟩ pyramids	colour purple (lattice constant a = 4.151 A); colour blue (lattice constant a = 4.155 A)	[26]

The control of crystal growth processes is complicated by the need to monitor and control several factors within closely specified limits: the rates of evaporation, the concentrations of the initial components in the carrier gas, the temperature gradient, etc. Data on the preparation of LaB_6 monocrystals by the gas-phase method are shown in Table 1.

The possibility of growing oriented and regular whisker structures of various elements and compounds by a gas-phase method, using Δc transport, is of great practical interest.[24]

The results in Table 1 show that LaB_6 monocrystals produced by the gas-phase method are usually facetted, and grow preferentially in a ⟨100⟩ direction. However, they tend to be small, and difficult to use as single-crystal samples in physical experiments. Furthermore, their precise chemical composition has never been reported, except for a list of impurities.[26] The same paper[26] gives the lattice constants of the LaB_6. Most other reports merely describe the colour of the crystals, which varies from purple to blue, the latter being ascribed to an excess of boron in the sample. However, this interpretation cannot be tested unambiguously because of the lack of chemical analyses. In view of the relatively low temperatures and other conditions used in the gas-phase method, and noting the data on the homogeneity region in Fig.1, it would appear that stoichiometric LaB_6 crystals can be produced, in principle, by this method. The main difficulty here is the need for exact control over the initial concentrations, which determine the La : B ratio in the monocrystal, and also the need for fine adjustment of many other factors (mentioned above) known to affect the stoichiometry of the growing LaB_6 crystals.

Another shortcoming of the gas-phase method (especially for the growth of crystals by using chemical reactions) is the possibility of co-depositing impurity phases such as boron with the LaB_6. As reported,[26] this danger can be avoided by using a BCl_3 concentration much lower than the value corresponding to the stoichiometric ratio $BCl_3/LaCl_3 = 6$. The coprecipitation of boron is entirely suppressed at $BCl_3/LaCl_3 < 2$.

The gas-phase method has not so far produced monocrystals of adequate quality and size. However, further developments (including the use of seed crystals) may result in the production of large and perfect LaB_6 crystals. Another promising line of research is aimed at the production of regular whisker structures of LaB_6, which may find practical application.[24]

2. The Liquid-phase Method

The liquid-phase method consists in passing the substance to be crystallised through a heated zone in which a temperature gradient is maintained, or in moving the zone relative to the sample. The compound, which can enter the zone either in the liquid or in the solid state, is first melted and then crystallised. The wide variety of possible technological variants of this method has led to the development of a large number of different techniques for growing single crystals.[22]

Only the zone melting method has been used for growing monocrystals of LaB_6, in the crucible-free form which avoids contact between the hexaboride melt and any container material. Data on the preparative conditions and characteristics of LaB_6 monocrystals prepared by zone melting are summarised in Table 2. The ingot for zone melting is previously prepared as a rod of the required diameter: the quality of the final product is largely determined by the composition and purity of these ingots. Various heating methods are used to generate the molten zone in the sample. Thus, relatively large (4–7 mm in diameter) monocrystals (or polycrystalline ingots) have been obtained with high-frequency[27,31] or electron-beam heating.[21] Thinner monocrystals (~1 mm diameter or less) have been prepared successfully by electric arc or laser methods of heating.[28] Dissociation and evaporation of the LaB_6 are avoided by carrying out the zone melting operation in an atmosphere of purified gas (usually argon).[27–30] Nitrogen, hydrogen, and helium have also been used.[21] The concentration of impurities can be lowered to the 10^{-3}–10^{-4}

wt.% level by repeated zone passes (see Table 2). It is reported[29] that a single zone pass can lower the impurity concentration (transition metals of Groups IV–VIII, Cu, Al, Ca, etc.) by a factor of 13–69, i.e. almost to the 10^{-2}–10^{-3} wt.% level, increasing to a factor of 315 (10^{-3} wt.%) after three passes.

Table 2. Preparation of LaB_6 monocrystals by the liquid phase (zone melting) method.

Preparative conditions			Characteristics of the monocrystals		Refs.
composition of initial billet c_{Σ}^{P}, wt.%	atmosphere; pressure, mmHg	formula	impurities, wt.%	growth direction; crystal size, mm	
LaB_6: 99.9	Ar; $1.1 \cdot 10^4$	LaB_6	non detected (3 zone passes)	not determined; $l = 60$, $d = 7$	[27]
$LaB_6 > 99.0$; $LaB_6 + (1.6-2)$	N_2; 20	La_xB_6, where $0.85 < x < 1.0$	$c_{\Sigma}^{P} < 0.1$ (microprobe) (1 zone pass)	not determined; $l = 25$, $d = 3.6$	[21]
LaB_6; $c_{\Sigma}^{P} = 0.485$	Ar; 760	–	$c_{\Sigma}^{P} = 0.043$ (2 zone passes)	⟨100⟩; $l = 60$, $d = 1.1$	[28]
$LaB_{6.00\pm0.03}$; $LaB_{5.99}$ and $LaB_{5.81}$	Ar; 52	$LaB_{6.00\pm0.15}$, $LaB_{5.86}$, $LaB_{5.72}$	$c_{\Sigma}^{P} = 0.0045$ (3 zone passes)	⟨100⟩; $l = 23-26$, $d = 0.25-1.50$	[29, 30]
$c_{\Sigma}^{P} = 1.125$	inert gas	LaB_6	$c_{\Sigma}^{P} = 0.015$	not determined; $l = 120$, $d = 7$	[31]
La + B; $c_{\Sigma}^{P} = 1.6$	Ar; 760	$LaB_{5.9}$, LaB_6	$c_{\Sigma}^{P} = 0.01$ (3 zone passes)	deviation from ⟨111⟩ 5°; $l = 120$, $d = 10$	[32, 33]

Notes: c_{Σ}^{P} is the total impurity concentration; l is the length and d is the diameter of the crystal.

In most of this work the initial LaB_6 had a stoichiometric composition. However, some workers used specially prepared initial samples which were deficient in lanthanum (i.e. contained added boron). In this way it was shown[21] that in order to produce good-quality billets boron powder must be added to the LaB_6 powder (2 mole boron to 1 mole LaB_6). The resulting monocrystals were of good quality, but they contained an excess of boron as well as the LaB_4 phase. The presence of LaB_4 can be attributed to the high rate of crystallisation used in those experiments,[21] which was an order of magnitude greater than normal values.

The LaB_4 had an oriented distribution, and its presence had almost no effect on the sharpness of the Laue diagrams of the LaB_6 monocrystals. A seed crystal containing an excess of boron (86.9% B) was used[28] in addition to seeds of stoichiometric composition. By studying the melting points of the samples it was concluded that the composition of the crystals corresponding to the highest melting point is shifted from the stoichiometric value towards the boron-rich side. This observation anticipated the publication[5] of the phase diagram of the La–B system. In addition, the LaB_4 phase was detected in samples prepared from billets of stoichiometric composition. Its presence was attributed to incongruent melting of the LaB_6.

As was stated above, according to data[5] obtained by the liquid-phase method (see Fig.1), the preparation of stoichiometric LaB_6 by this method (including zone melting) is impossible even when non-stoichiometric initial ratios of La to B are used to allow for differences in evaporation rate at the growth temperature. However, some workers[27,31,33] have assigned the formula LaB_6 to their lanthanum hexaboride crystals on the basis of chemical analysis (and within the precision of that method, see Table 2). We should stress that, unfortunately, the exact quantities of B and La in the resulting LaB_6 monocrystals are not stated in those papers, and no indication is given of the precision of the chemical analysis. Therefore it is difficult to establish the exact ratio of B to La in those samples and the exact formula of the hexaboride.

This shortcoming is not found in an analytical investigation[30] specially aimed at determining the stoichiometry of the grown LaB_6 crystals (see Table 2) and at identifying the impurities in the samples. All the monocrystals were found to be deficient in boron both in respect of their stoichiometric composition and in respect of the composition of the initial ingot, but they were free from inclusions of the LaB_4 phase. Relatively large amounts of carbon were detected in the crystals. The low boron content was attributed[30] to the formation of a compound between boron and carbon by the reaction of carbon with the LaB_6 melt (but no experimental evidence for this suggestion is given). On the evidence of chemical analysis and density data these workers concluded that the boron sublattice contained defects and that La atoms could be accommodated in the sites of the missing octahedra of boron atoms.

Thus the liquid-phase method can be used to prepare reasonably large monocrystals of high purity, but it has serious disadvantages such as a variable and non-stoichiometric composition of the resulting LaB^6 crystals and the presence (in some cases) of LaB_4 and B inclusions.

3. Crystallisation from Solutions

The solution method consists in the mass (or seeded) crystallisation of refractory compounds from metallic, salt, or hydrothermal solutions. The crystallisation takes place at a fixed (or variable) solution supersaturation, produced by evaporating the solvent or by lowering the temperature and by the corresponding decrease in solubility of the substance to be crystallised. The crystallisation is controlled by using a seed crystal immersed in the solution, and by establishing special regimes of solvent evaporation and cooling the system or adding feed material to it.[22]

The variants of this method differ in the nature of the solvent (elements, compounds, metals, salts) and in its relationship to the solute (i.e. in its ability to form compounds with it).[22] One of the main attractions of the solution method is the possibility of obtaining different morphological modifications of the monocrystals (needles, plates, isometric crystals), and also the relatively low temperatures of the growth processes and their technological simplicity. So far, only crystallisation from solutions in metallic melt and electrocrystallisation have been used to prepare monocrystals by the solution method. Information on the crystals prepared by these methods is given in Table 3.

Let us examine in greater detail the solution method, which appears to offer the most promising possibilities for the production of stoichiometric LaB_6 crystals. To control the crystallisation of LaB_6 from solution in Al we need information on the phase equilibria in the ternary La–B–Al system at different temperatures, and also data on the polythermal section of the LaB_6–Al phase diagram. If these data are available we can establish the following:

1) the temperature dependence of the solubility of LaB_6 in an Al melt;

2) the phase relationships and interconversion during crystallisation.

However, the phase diagram of the La–B–Al system has not so far been determined. The reported[46] isothermal section of the phase diagram at 873 K shows that ternary compounds are not formed on this section and that the LaB_6 is in equilibrium with the Al, indicating the possibility of preparing LaB_6 crystals from the Al melt. Since the LaB_4–Al equilibrium does not appear on the isothermal section, the LaB_4 phase cannot crystallise and contaminate the LaB_6 crystals. There is no information on the temperature dependence of the solubility of LaB_6 in an aluminium melt: the composition of the initial charge is usually calculated approximately by equating the solubility of LaB_6 to that of boron in aluminium at the given temperature. This estimate is only a rough approximation, and apparently too high, but at present we have no better way of defining the crystallisation regime of the LaB_6.

An overall representation of the crystallisation regimes can be based on the data in Fig.2, which shows a polythermal section with a metastable region in the phase diagram of refractory compound (MN)–solvent metal (R) systems, together with possible variants of the mass crystallisation regime.

The metastable region, defined by the full curves, is divided into two parts by the dot-and-dash curves, corresponding to the spontaneous formation of singlet nuclei (part *I*, temperature range T_1–T_2) and to massive nucleation (part *II*, range T_2–T_3), but not so massive as in the labile region below T_3. After being heated to the required temperature and held at that temperature for the time needed for the synthesis and homogenisation of the molten solution the system can be cooled according to several regimes, of which the most effective is $A_1B_1C_1D_1$. After a hold at the temperature A_1 the system is rapidly cooled to the temperature B_1 to form a relatively small number of nuclei, then the temperature is raised to C_1 to redissolve the more unstable nuclei (in order to decrease the number of nuclei and thus obtain larger crystals), and lastly the system is cooled along the line C_1D_1, which is parallel to the solubility curve of the crystallising compound. Other regimes (see Fig.2) yield smaller and less perfect monocrystals, and are only used for special reasons.[47]

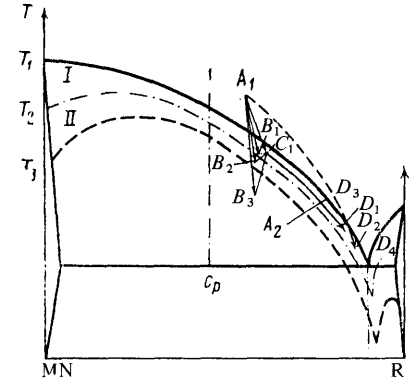


Figure 2. Metastable region (diagrammatic) in a polythermal section of the MN–R phase diagram and mass crystallisation regimes (from Ref.47).

LaB_6 monocrystals of stoichiometric (or near-stoichiometric) composition are obtained by crystallising the system by the solution method according to the LaB_6–Al polythermal section (Fig.3), starting from the temperature 2073 K at which the left-hand edge of the homogeneity region begins to follow the stoichiometric composition towards lower temperatures. This

Table 3. Preparation of LaB_6 monocrystals by the solution method.

Initial components			Preparative conditions			Characteristics of monocrystals			Refs.
Composition (wt.%); weight of solvent (g)	purity of B and La (wt.%); B/La ratio	*c*, wt.%	*T*, K	*t*, h	*v* K h^{-1}	shape and size of crystals, mm	method of analysis; formula	c^p $c^p_{\sum}$, wt.%	
Al (99.9999) —	B (99.99), La (99.9); 6:1	13.35	1773	0.16	25	needles 5.0–7.0 × 0.1 × 0.1; plates 2.00 × 3.00 × 0.05; cubes	—	0.01	[34.35.36.37]
Al(99.9); 90—140	B (99.99), La (99.9); 4.98:1	2.4÷3.6	1473	5÷10	6.2÷75	needles 5.0 × 0.5 × 0.5; plates; cubes	—	0.045	[38]
Al(99.8); 58	B (99.8), La 99.5) 5.8:1	3.06	1773	8	30	needles; plates; cubes	—	0.005—0.01	[39]
Al(99.99); —	B (>99), La (>99); 6:1 or 12:1	5÷10	1573—1673	2÷10	—	needles 10.0 × 0.5 × 0.4; plates 6.00 × 7.00 × 0.15; cubes 1.90 × 0.85 × 0.85	chemical analysis**: $LaB_{5.86}$ (31.0 wt.% B); $LaB_{6.04}$ (32.0 wt.% B)	0.056 (Al)	[40—43]
Al; 41	B (99.9), La_2O_3; (4÷8):1	10	1773	120	5÷20	needles 5 × 1 × 1; plates 2.0 × 2.0 × 0.1; cubes 1 × 1 × 1	microprobe: (30.00 ± 0.08 wt.% B)	—	[44]
*—	—	—	1073	200÷300	no cooling	cubes 6 × 6 × 5	microprobe; $La_{0.67}B_6$÷$La_{0.87}B_6$	—	[45]

Symbols: *c* is the concentration of LaB_6 in solution, *t* is the hold time, *v* is the cooling rate.

*Crystals prepared by electrocrystallisation from molten salts (melt composition, mole %: La_2O_3 0.1–4, B_2O_3 33.5, Li_2O 31.2, LiF 33.1.

**The calculated boron content of LaB_6 is 31.8 wt.%.

property of the system imparts some substantial advantages to the solution method as compared with other methods of producing LaB_6 crystals of stoichiometric composition.

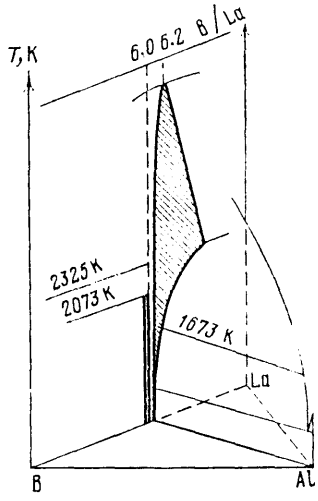


Figure 3. Polythermal section (diagrammatic) of the LaB_6–Al phase diagram (from Ref. 47).

The LaB_6 crystals are usually prepared as follows. Known weights of boron and lanthanum (in stoichiometric proportions) are placed in an alundum crucible or boat together with the aluminium, heated in an argon atmosphere to the required temperature, held at this temperature for several hours in order to homogenise the melt, and after rapidly lowering and again raising the temperature the system is brought to 873 K by forced cooling (see Fig. 2).[47] The fundamental condition for successful crystallisation is that the point $B_{1(2)}$ must always lie within the metastability region (preferably, in its upper part). The following mass crystallisation regimes can be defined (Fig. 2): $A_1B_1C_1D_1$ (the optimum); $A_1B_2C_1D_1$ (a possible regime for a broad homogeneity region of the crystallising substance); A_1D_2 (an "incorrect" regime, leading to the deposition of very small crystals); $A_2D_3D_4$ (a possible regime for a low synthesis temperature).

After being cooled the aluminium ingots are dissolved in dilute HCl, NaOH, or KOH to isolate the LaB_6 crystals. La_2O_3 can be used as one of the initial components instead of metallic La: in this case the reaction $La_2O_3 + B + Al \rightarrow LaB_6 + Al_2O_3 +$ other products takes place in the aluminium melt.[44,48]

In the temperature range 1473–1773 K (see Table 3) the LaB_6 crystallises from solution in an Al melt in three morphological modifications: needles, plates, or isometric cubic crystals (Fig. 4*a* and 4*b*), the needles and plates being much larger than the cubic crystals. It was reported[38] that under stated experimental conditions (see Table 3) the needle-like crystals greatly outnumber those of other morphologies. For example, at a cooling rate of 75 K h^{-1} the numerical ratio of the crystals of different habit (needles : plates : cubes) was 76 : 23 : 1. It is also reported[43] that this ratio depends on the concentration of LaB_6 in the Al: increasing the concentration increases the proportion of platelets in the crystals.

From the Laue patterns of the crystals it was concluded[49] that the plates and needles have {100} cube faces, i.e. the plates have a large (100) face (several mm^2 in area) and the needles are elongated in the <100> direction. This is confirmed by data on the etching behaviour of the monocrystals.[38,42] Some crystals have smooth faces, others show conical projections and growths steps, and skeletal growth forms are also found (in the shape of hollow cubes and needles), denoting a high degree of supersaturation during the growth (Fig. 4*b*). It was shown[49] that many monocrystals have a block structure, with a maximum mis-orientation of 2° in platelets and much smaller (~10′) in needles (the mis-orientation of the blocks was calculated from photographic enlargements of the Laue spots).

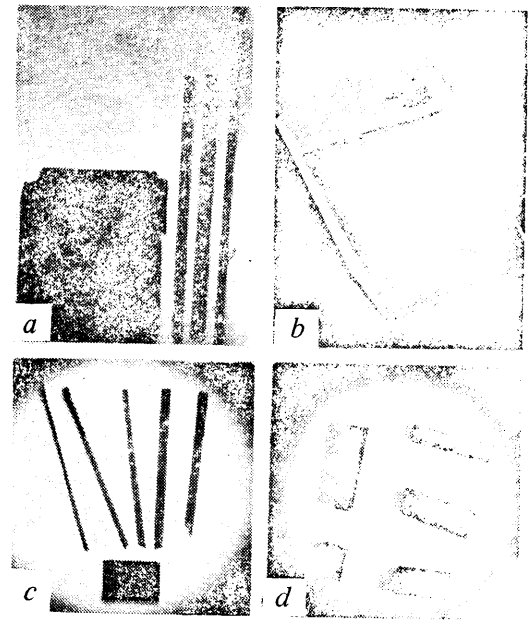


Figure 4. General shape of monocrystals of lanthanum hexaboride and of solid solutions of the $La_{1-x}M_xB_6$ type crystallised from aluminium: *a*) needles and plates of LaB_6; *b*) cubic LaB_6 crystals; *c*) $La_{1-x}Ce_xB_6$ solid solution; *d*) $La_{1-x}Tb_xB_6$ solid solution; magnification x6 (*a*, *c*, *d*) and x500 (*b*).

The composition of the LaB_6 monocrystals was determined quantitatively only in two investigations,[42,44] aiming to establish the effect of the B/La ratio in the initial ingot on the composition of the resulting crystals. In one of these studies[42] chemical analysis showed that the composition of the crystals obtained for a stoichiometric initial ratio of the components generally corresponds to the formula $LaB_{6.0}$. An initial ratio of 12 : 1 yields crystals deficient in boron ($LaB_{5.86}$). Other workers[44] varied the B/La ratio between 4 : 1 and 8 : 1 but could not detect any difference between the compositions of the resulting crystals. The reported composition in this case corresponded to a deficit of boron in the lanthanum hexaboride crystals. We should stress that in spite of the use of an excess of boron in the initial charge there has not been a single report of the deposition of a LaB_9 phase by crystallisation from an Al melt.

Aluminium inclusions have been detected in some LaB_6 crystals.[38,42] This type of solvent entrainment is observed at high rates of growth of the crystals from solution.[50] The crystallisation regime should be defined so as to avoid the formation of extraneous inclusions.

The crystallisation from Al solutions yields lanthanum hexaboride crystals of various colours: from a bright purple to violet and blue. There have been attempts to associate the blue colour with the presence of finely divided inclusions of free boron[13] or with a small lanthanum defect[3,6,19] (for example, the La content was found[6] to be 66 wt.%). However an X-ray microprobe analysis of crystals of different colour prepared by the solution method detected identical boron concentrations in all the crystals.[44] It was reported[49] that after brief etching in dilute HNO_3 all the crystals display a bright purple colour gradually turning to blue on long exposure to air. The conclusion[44,49] was that the differences in colour between the crystals are due to differences in the state of the surface (mainly, the presence of an oxide film).

The total impurity content of these LaB_6 monocrystals according to spectrographic analysis is 0.005–0.05 wt.% (see Table 3), i.e. fully comparable with the purity of the crystals prepared by zone melting (Table 2). Obviously, even purer crystals can be prepared from purer starting materials by exploiting the distribution coefficients of the various impurities.

LaB_6 monocrystals containing the ^{10}B and ^{11}B isotopes, needed in various investigations,[49] have also been prepared by crystallisation from a solution in molten Al.

In an attempt to improve the emission properties of LaB_6 cathodes, monocrystals of solid solutions of the type $La_{1-x}\cdot M_xB_6$ have been prepared,[40,44,48,51,52] where M is a rare-earth (Ce, Gd, Tb, Pr, Nd, Sm, Dy, Y) or an alkaline earth metal (Ba), and x varies between 0.02 and 0.70 atom fraction. These are similar in size to the pure LaB_6 crystals (needles and platelets, see Figs. 4*c* and 4*d*). It was reported[44] that the composition of the solid solution crystals is not exactly correlated with the initial component ratio. The discrepancy between the initial LaB_6/MB_6 ratio and the composition of the crystals can be as high as ±15 mole % in some crystals. Other workers[52] find this scatter to be less than 8 at.%.

Another method (electrocrystallisation from molten salt solutions) has been used to prepare fairly large cubic monocrystals of LaB_6 (see Table 3). The most significant feature of this method is that electrolysis of the molten salts (or oxides) is carried out at constant temperature. The driving force of the crystallisation process is the applied potential gradient. Electrolysis has been carried out at a constant voltage between 1.85 and 2.1 V, which gives the cathodic current density (20–40 mA cm^{-2}) needed for crystal growth. Unfortunately, the composition and impurity content of the LaB_6 crystals (grown on a seed) is not quoted,[45] and these results cannot be compared with those obtained by other methods.

A comparison of all the methods of preparing lanthanum hexaboride crystals (Table 4) shows that the highest temperatures are used in the liquid-phase methods; in the gas-phase and the solution methods the maximum temperatures are similar, and lower than T_m for lanthanum hexaboride by almost a factor of two; the liquid-phase method offers the highest rate of growth of monocrystals. Though each of these methods (in principle) can be used, with appropriate seeds, to grow single crystals oriented in any required crystallographic direction, this has been achieved, in practice, only in the liquid-phase method. Different morphological modifications of idiomorphic monocrystals can be obtained only by the solution method. The limiting impurity concentrations in monocrystals prepared by the different methods are approximately equal. Allowing for the shape of the LaB_6 homogeneity region (especially in crystallisation by the solution method) leads to the production of stoichiometric or very nearly stoichiometric monocrystals. The liquid-phase method often produces inclusions of LaB_4 and B, while inclusions of Al are obtained when the solution method is used.

The most perfect monocrystals are grown by the solution method, with the smallest block misalignment and the lowest dislocation density. Single crystals of a prescribed shape can be prepared only by solution and by liquid-phase methods (in the latter case, by using Stepanov's profiling method[53]). These aspects should not be forgotten when comparing the future prospects of the various methods. On the whole it is difficult to identify any one method as superior to all others. Each method has its advantages and disadvantages, and each can yield monocrystals of adequate quality. In view of the practical requirement for monocrystals in needle or platelet form for the preparation of hot or cold emission cathodes, and of the difficulty of growing those crystals by the liquid-phase method, the solution method of growing LaB_6 crystals of stoichiometric composition offers some advantage over the other methods.

Table 4. Comparison of methods of preparing LaB_6 monocrystals.

Parameters	Methods		
	gas phase	liquid phase	solution
Preparative conditions			
Temperature range, K	1273 - 1723	above 2988 (degree of superheating not quoted)	1073 - 1773
Growth time or rate of pulling (or cooling)	0.5 - 3 h	18 - 420 mm h^{-1}	5 - 75 K h^{-1}
Other features and prospects of the method	preparation of oriented regular structures	growth on seeds	growth of crystals in a prescribed orientation; electrocrystallisation
Characteristics of resulting monocrystals			
Maximum size, mm	$l = 5$ (needles), $d = 2 \times 10^{-5}$	$l < 120$ (rods), $d = 1 - 10$	needles 10.0 × 0.5 × 0.4; platelets 6.00 × 7.00 × 0.15; cubic crystal 6 × 6 × 5
Impurity content, wt.%	at the limit of sensitivity of the microprobe	$10^{-1} - 10^{-4}$	Al up to 2×10^{-1} – $(5-10) \times 10^{-3}$
Structural perfection (misorientation of the blocks)	no data	between 20″ and a few degrees	platelets up to 2″, needles up to 10″
Dislocation density, cm^{-2}, and face	$10^4 - 10^5$; (100)	$10^6 - 10^7$; (100)	$10^3 - 10^5$; (100)
Possibility of preparing monocrystals of stoichiometric composition	yes	no	yes

These conclusions are confirmed by X-ray structural studies[17,54,55] of three LaB_6 monocrystals prepared by the solution method with different B/La ratios in an Al melt and at different temperatures (B/La = 9:1 and 5:1 at 1673 K; B/La = 9:1 at 2073 K). The results on the crystal structure of LaB_6, shown in Table 5, were unexpected. Instead of defects in the lanthanum sublattice, which could have been expected in boron-rich compositions,[3,10] full occupancy of the lanthanun positions and a small defect density in the boron sublattice were observed in all three crystals, irrespective of their composition. It follows that the data on the homogeneity region

of LaB_6 (see Fig.3), at least those at 2073 K and below, need to be re-examined: it appears that the boundary coinciding with the line of stoichiometric composition should be the right (rather than the left) solidus line. With this exception the shape of the homogeneity region should be as outlined in Ref.6.

Table 5. Data on the structure of LaB_6 (from Refs.54 and 55).

Structure parameters	Crystal No.1	Crystal No.2	Crystal No.3
Position of boron atom, x_B	0.19956 (16)	0.19957 (15)	0.19948 (14)
Occupancy and position factor of the boron, %	96.4 (7)	97.2 (5)	98.2 (5)
Isotropic temperature factor of the lanthanum U_{iso}, $Å^2$	0.00535 (3)	0.00551 (2)	0.00525 (2)
Anisotropic temperature factor of the boron, $Å^2$: U_{11} $U_{22} = U_{33}$	0.0031 (2) 0.0044 (2)	0.0032 (2) 0.0046 (1)	0.0031 (2) 0.0046 (1)
Divergence factor R, %	1.36 (935 reflections)	1.10 (1224 reflections	1.15 (1190 reflections)
B/La atomic ratios: from X-ray analysis data from chemical analysis data	5.76 5.7	5.80 —	5.86 6.8

Notes. The standard errors are shown in brackets. The following initial ratios in the melt and temperatures were used: crystal No.1, B/La = 9:1, T = 1673 K; crystal No.2, B/La = 5:1, T = 1673 K; crystal No.3, B/La = 9:1, T = 2073 K.

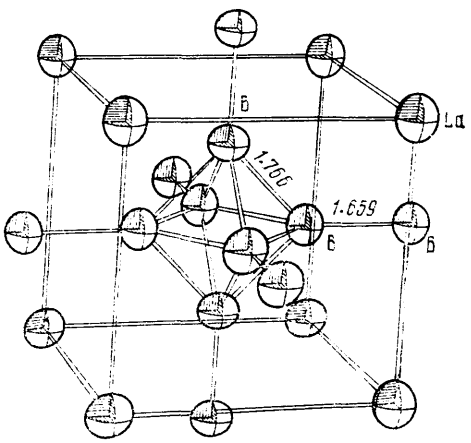


Figure 5. Crystal structure of LaB_6; the thermal vibration ellipsoids of the atoms are taken from Refs.54 and 55.

Another important result of these studies[54,55] is the recognition of a large anisotropy in the thermal vibrations of the boron atoms (see Fig.5 and Table 5). It is clear that the thermal vibrations of the boron atoms are weaker in the direction of the bond between octahedra than in the direction of the bonds within the octahedron. This conclusion is consistent with the results of studies of LaB_6 monocrystals by Raman spectroscopy,[56,57] according to which the force constants of the B–B bonds between octahedra and within the octahedra are 2.18 and 1.28 mdyn $Å^{-1}$ respectively. We should also stress that the amplitude of the thermal vibrations of the La atoms is greater than that of the B atoms (see Table 5). This suggests a rigid boron sublattice with lanthanum atoms vibrating relatively freely in its interstitial sites. These aspects of the crystal structure of lanthanum hexaboride are responsible for many of its properties, discussed in the next section.

IV. SOME PROPERTIES OF LANTHANUM HEXABORIDE MONOCRYSTALS

In this section we shall aim as far as possible to discover the relationship between the properties and the composition of LaB_6 monocrystals.

1. Electrophysical Properties

The electrophysical properties of LaB_6 monocrystals have been studied mainly on samples prepared by zone melting.[27,58,59] The results confirm the metallic nature of LaB_6, previously established for polycrystalline samples.[10] Hall effect measurements on samples of two types (prepared with 1 pass and 3 passes of the molten zone respectively) gave the same value of the Hall constant (R_H) in both cases: in other words, this constant is independent of the purity of the crystals.[27] The carrier concentration calculated from R_H is ~1 electron per La atom, which agrees with the band structure of the hexaborides of tervalent rare-earth metals suggested in the early publications.[60,61] An important characteristic of LaB_6 monocrystals is the ratio of the electrical conductivities at 300 and 4.2 K ($\rho_{300}/\rho_{4.2}$). We know that the electrical conductivity of metals at room temperature is determined mainly by the scattering of the conduction electrons on acoustic phonons, whereas at liquid-helium temperatures it is determined by scattering at impurity atoms and lattice defects.[62] Therefore this ratio is very sensitive to the quality of the crystals: the fewer impurities and defects are present in the crystal, the lower will be the residual electrical resistance $\rho_{4.2}$, and the higher the ratio $\rho_{300}/\rho_{4.2}$. Thus, for melted polycrystalline samples (1 zone pass) containing 10^{-1}–10^{-2} wt.% of impurities the ratio was 20–45,[27,59] whereas for the purer monocrystals (3 zone passes) containing ~10^{-3}–10^{-4} wt.% of impurities the ratio was 200–450,[27,58] and even as high as 740.[63] In monocrystals prepared by the solution method the ratio $\rho_{300}/\rho_{4.2} \approx 200$ [35] corresponds to the lower limit for the zone-melted crystals. However, we should remember that the error in measuring this quantity may be large in the case of small crystals.

A study[58] of the temperature dependence of the electrical resistance of a zone-melted monocrystal ($\rho_{300}/\rho_{4.2} = 450$) in the range 360–4.2 K has shown the need to allow for the contribution from the scattering of electrons on optical phonons, which becomes appreciable at ~100 K. At 300 K this contribution accounts for ~30% of the total resistivity of the LaB_6. The scattering of electrons on optical phonons is an important difference between LaB_6 and metallic elements, which confirms the ionic nature of the interactions between the boron and lanthanum sublattices.[60] A study of the dynamic resistance of a LaB_6 monocrystal at 1.7 K by the point contact spectroscopy method confirmed the predominance of electron–phonon interaction processes in the scattering of electrons.[64]

Experimental studies of magnetoresistance and of the de Haas–van Alphen effect have been made on monocrystals prepared by solution and liquid-phase methods,[35,63,65] using models of the Fermi surface for LaB_6 which were consistent both internally and with calculations of the band structure of LaB_6.[66,68] According to those measurements[35,63,65] the conduction band of LaB_6 is very wide, and the conduction electrons have a negligibly small *s* character owing to the hybridisation of the 5*d* orbitals of the lanthanum atoms with the 2*s*–2*p* orbitals of the boron atoms. A study of the energy structure of the valence band by determining the angular dependence of the photo-emission from the (100) faces of a LaB_6 single crystal prepared by zone melting[69] revealed the presence of several sub-bands in positions agreeing to within ~0.5 eV with calculated results.[67]

Information on the band structure can also be obtained from the reflectance spectra, which have been studied on polycrystalline samples prepared by zone melting and on films of LaB_6 in the energy range 0.05–6 eV.[25,70–74]

2. Optical Properties

The optical properties of LaB_6 monocrystals were first studied over a wide range of energies (0.05–40 eV) on laminated crystals (mosaics of platelets) prepared by the solution method.[75,76] The reflectance spectrum of LaB_6 (curve *1* of Fig. 6*a*) shows a deep minimum at an energy of 2.1 eV, due to the interaction of light with the conduction electrons. It corresponds to a sharp maximum in the loss function ($-\mathrm{Im}\,\varepsilon^{-1}$, curve *3* of Fig. 6*b*). At energies greater than 2.1 eV we observe a steep increase in the imaginary part of the dielectric constant ε_2 (curve *2* of Fig. 6*b*), indicating band-to-band transitions (direct band gap) of the electrons from the valence band to the conduction band, whose lowest levels are filled with electrons. Hence the spectra of the optical constants in present energy range are determined both by the conduction electrons and by the inter-band transitions, and therefore the frequency ω_{min} corresponding to R_{min} is not equal to the plasma frequency ω_p. By separating the contribution from the conduction electrons (ε^e) (curve *4* of Fig. 6*b*) to the real part of the dielectric constant ε_1 (curve *1* of Fig. 6*b*) we can determine the true value of the plasma frequency ω_p. Inspection of the characteristic loss function ($-\mathrm{Im}\,\varepsilon^{-1}$, curve *3* of Fig. 6*b*) establishes the presence of a broad maximum at energies of 27–30 eV, due to the onset of plasma vibrations of the valence electrons. The calculated energy of these vibrations is 20 eV, i.e. we find (as in the case of the conduction electrons) a shift in the energy of the plasma vibrations as a result of band-to-band transitions. The similarity between the spectral dependence of the characteristic loss functions for LaB_6 and for the betarhombohedral modification of elemental boron suggests that the role of the boron atom in the formation of the spectrum of the hexaboride is dominant in the high-energy region.[76]

The boron sublattice of LaB_6 also determines the form of the Raman spectrum, which was studied on monocrystals prepared by zone melting.[56,77] The spectra were measured on polished (100) and (111) surfaces of monocrystals. Several peaks were observed, and assigned to three modes of lattice vibration active in the Raman region:

	From Ref.56	From Ref.77	
A_{1g}	1258 cm^{-1}	1262 cm^{-1}	B–B bond
E_g	1120 cm^{-1}	1138 cm^{-1}	B–B bond
F_{2g}	682 cm^{-1}	688 cm^{-1}	distortion of the boron sublattice

A peak at 214 cm^{-1}, attributed to scattering on defects of the crystal structure, was also observed.[77] A similar peak at 208 cm^{-1} was observed[58] in $La_{1-x}Ba_xB_6$ monocrystals (where $x = 0.02–0.046$) and attributed to the local perturbation of the symmetry produced by the replacement of La by Ba.

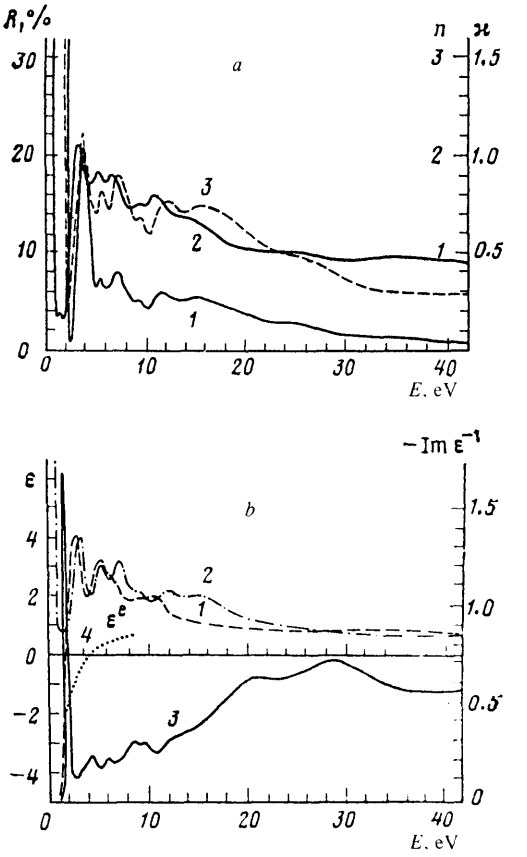


Figure 6. Dependence of the optical constants of LaB_6 on the energy *E* of the incident radiation;[75,76] a) reflectance *R* (*1*), refractive index *n* (*2*), and extinction coefficient κ (*3*); b) real (ε_1, *1*) and imaginary (ε_2, *2*) parts of the dielectric permeability function and of the loss function ($-\mathrm{Im}\,\varepsilon^{-1}$, 3).

3. Mechanical Properties

The elastic properties of LaB_6 are also determined mainly by the boron sublattice, as shown by measurements of the elastic constants of LaB_6 on samples cut in the <001>, <110>, and <111> directions from single crystals prepared by zone melting:[57]

$$C_{11} = 45.33 \times 10^{10}\ \mathrm{Pa}$$
$$C_{12} = 1.82 \times 10^{10}\ \mathrm{Pa}$$
$$C_{44} = 9.01 \times 10^{10}\ \mathrm{Pa}$$

The anisotropy factor is $A = 2C_{44}/(C_{11} - C_{12}) = 0.41$. Young's modulus, calculated for the <100> direction, is 45.18×10^{10} Pa, while the value calculated from the force constants of the bonds in the boron sublattice between octahedra and within the octahedra[56] is 40×10^{10} Pa. This good agreement is interpreted[57] as evidence that the elastic constants of LaB_6 are determined by the rigid boron sublattice. The large ionic

contribution to the bond between the boron and the metal sublattice accounts for the anisotropy factor $A < 1$ in LaB_6 (a value usually found in ionic crystals).

Young's modulus for polycrystalline LaB_6 prepared by zone melting is 39.24×10^{10} Pa,[78] i.e. it is slightly lower than for the monocrystals. It is interesting to note that a theoretical calculation of Young's modulus for LaB_6 [79] gave a value of 47.09×10^{10} Pa, i.e. in these monocrystals the measured Young's modulus is very close to the theroretical value.

Data on the micro-hardness of LaB_6 monocrystals prepared by various methods are shown in Table 6. They cover a wide range, but since the measurements were carried out with different loads it is difficult to compare the results. There is an obvious tendency for the micro-hardness to decrease with increasing load on the indentor. Furthermore, the micro-hardness measured with a Vickers pyramid (H_V) is different from that measured with a Knoop pyramid (H_K), which is a characteristic of brittle materials.[80] The brittleness of LaB_6 is found to be similar to that of silicon.[80]

Table 6. Micro-hardness of LaB_6 monocrystals measured by different methods.

Method of preparation; crystal form; face	Micro-hardness, kg mm^{-2}		Load on indentor, g	Refs.
	H_V	H_K		
Gas phase; needles; (100)	3400—3700	—	50	[26]
Solution; platelets, needles; (100)	2620±80	—	100	[42]
Liquid phase	2020	—	300	[21]
Liquid phase; (100)	—	1850±90	510	[80]
(110)	—	1550±60		[80]
(111)	—	1490±70		[80]
Solution; (100)	—	2450	50	[81]
ditto	—	1980±130	200	[81]
"	—	1720	400	[81]

The anisotropy of the micro-hardness has been studied on monocrystals prepared by zone melting[80] and by the solution method.[81] In a study[81] of the anisotropy of the hardness (polar anisotropy) on the (100) face the maximum hardness was found with the longer diagonal of the indentor oriented in the <010> direction, and the minimum in the <011> direction (the difference between the two measurements was 300 kgf mm^{-2}). Ref. 80 describes a study of the reticular anisotropy of the micro-hardness, showing that the maximum value of H_K occurs in the (100) plane, where the density of La atoms is a maximum, and the minimum occurs in the (111) plane.

4. Emission Properties

Because of the extensive use of LaB_6 cathodes in various types of electronic device, data on the thermo-electronic work function ϕ of the material are of interest. The cathode current density I_C during thermo-electronic emission is described by the Richardson–Dushman equation

$$I_c, \text{ A cm}^{-2} = AT^2 \exp(-e\varphi/kT) \quad (1)$$

where T is the temperature of the cathode (K), e is the charge on the electron, and A is the Richardson constant. The work function ϕ can be determined by two methods: 1) graphically, from the slope of the linear plot of $\lg(I/T^2)$ against e/kT (we shall call this value of the work function ϕ_R), and 2) by calculation from formula (1), assuming a value of the Richardson constant of $A = 120$ cm^{-2} K^{-2} (we shall call this value ϕ_{ef}). Both ϕ_R and ϕ_{ef} values are used in published work, though according to some workers[83] the use of ϕ_{ef} is preferable.

The results of various workers on the work function of polycrystalline LaB_6 and of LaB_6 monocrystals have recently been critically examined in Refs. 83 and 84 respectively.

Storms and Mueller[83] examine in detail the various factors responsible for the large scatter of the measurements of work function on polycrystalline LaB_6: deviations from stoichiometry in the bulk of the sample, differences in composition of the surface whose emission is measured, the temperature of the experiment, and the hold time of the sample at this temperature, the presence of impurities in the sample and in the residual atmosphere, and many other factors. For polycrystalline samples of composition in the range $LaB_{5.85}$–$LaB_{6.50}$ the surface composition at 1500 K varied between $LaB_{6.032}$ and $LaB_{6.047}$, the work function ϕ_{ef} was 2.91–2.93 eV, and ϕ_R was 3.15–3.12 eV. Surprisingly, a further increase in the overall boron content produces an increase in ϕ_{ef} and a decrease in ϕ_R (a sample of composition $LaB_{8.6}$, with a surface composition $LaB_{6.1}$, gave $\phi_{ef} = 3.17$ and $\phi_R = 2.21$ eV).

Evidently, these factors must affect the measured work function also in the case of monocrystals. Furthermore, the work function of the LaB_6 sample depends on the crystallographic direction, as in metals with body-centred cubic, face-centred cubic, or close-packed hexagonal crystal lattice. Data on the emission properties of monocrystals prepared by liquid-phase and by solution methods are shown in Table 7. We note that the scatter in the ϕ values is large also in monocrystals. Nevertheless the anisotropy in the work function with respect to the crystal orientation is clearly observable: $\phi_{(100)} \leqslant \phi_{(110)} \leqslant \phi_{(111)}$.

Table 7. Work functions of different faces of LaB_6 monocrystals prepared by liquid-phase and solution methods.

(100)		(110)		(111)		Refs.
φ_R, eV	φ_{ef}, eV	φ_R, eV	φ_{ef}, eV	φ_R, eV	φ_{ef}, eV	
Liquid-phase method						
2.4±0.2	—	—	—	—	—	[85]
2.91	2.70	3.09	2.98	2.85	3.35	[21]
2.86±0.03	—	2.68±0.03	—	3.4±0.2	—	[86]
—	2.52±0.05	—	2.64±0.05	—	2.90±0.05	[84]
—	—	2.74	—	2.0	—	[87]
—	2.75	—	2.88	—	2.98	[31]
Solution method						
2.47±0.06	—	—	—	—	—	[36]
—	2.38	—	2.07	—	—	[37]
3	—	—	—	—	—	[88]
—	2.70±0.05	—	—	—	—	[89]
—	2.86±0.04	—	—	—	—	[52]
2.3±0.1	—	—	—	—	—	[90]

It would be interesting to compare the work functions of monocrystals differing in purity and in composition. Unfortunately, this comparison is possible only in a few cases because of the inadequate specification of the experimental materials in much of the published work. Thus, boron-rich crystals prepared by zone melting ($La_{1-x}B_6$) and having a high impurity concentration[21] have a higher work function (on all faces) than crystals with a boron deficit ($LaB_{5.86}$) containing very few impurities.[30,84] The work function of the (100) face of LaB_6 monocrystals[89,90] prepared by a solution method[37–39] and

containing ~10^{-2} wt.% of impurity is close to that of crystals prepared by zone melting and having a similar impurity concentration.[21,31]

By using modern methods of studying solid surfaces such as Auger electron spectroscopy (AES) and low-energy electron diffraction (LEED) the effect of impurities on the work function of LaB_6 monocrystals has been demonstrated more clearly. In particular, it has been shown[91] that the carbon present in the sample prepared by zone melting with one zone pass diffuses to the surface on heating the sample and forms a monolayer of graphite which is stable for a long time even at 1500 K. This effect increases the work function of LaB_6.

It has been shown[84,90,92] that carbon and oxygen are the main impurities on the (100), (110), and (111) surfaces of LaB_6 monocrystals. Their bond to the surfaces is fairly strong, and they are completely removed only by heating the sample to ~1700 K in a vacuum of 10^{-8}–10^{-10} mmHg. Studies of the oxidation kinetics at room temperature of clean (100), (110), and (111) surfaces of LaB_6 monocrystals showed that at oxygen pressures of 10^{-7}–10^{-9} mmHg O_2 adsorption raises the work function of these faces by 1.6, 1.3, and 1.1 eV respectively.[92–96] Raising the temperature to 1700 K strengthens the oxidation, and produces an increase of 2.4 eV in the work function of the (100) face[92] and a decrease in the emission current.[90,91] A large decrease in emission current is produced also by hydrogen, methane, and water vapour.[90] It has been established that rearrangement of the (110) monocrystal surface with formation of (111) facets takes place in an oxygen atmosphere at ~10^{-6} mmHg and 1700 K, leading to an increase in the work function of the (110) face and a decrease in emission current.[86,98]

Table 8. Atomic ratio B/La on the surface of different faces of LaB_6 monocrystals prepared by solution and by liquid-phase methods.

Face	B/La	Measurement method	Refs.	Face	B/La	Measurement method	Refs.
Solution method				Liquid-phase method			
(100)	2.3—2.6	AES	[36]	(100)	4.1±0.1	AES	[84]
(100)	2.33—2.60	AES	[92]	(100)	4.0	UPS	[101]
(100)	2.0	AES	[1]	(110)	5.4±0.1	AES	[84]
				(111)	5.9±0.2	AES	[84]

The nature of the work function anisotropy in different faces of the LaB_6 monocrystals is also of interest. Studies of these faces by AES, LEED, UPS (ultraviolet photoelectron spectroscopy), and XPS (X-ray photoelectron spectroscopy) have shown[36,84,87,92,93,99–101] that the Ba/La ratio on the monocrystal surface increases in the sequence (100) < (110) < (111) (see Table 8). The work function decreases in the same order, i.e. the greater the density of La atoms on the surface, the lower is the work function. This observation is unexpected, since the opposite effect is found on elemental metals: ϕ increases with the density of metal atoms on the surface. The explanation of this anomaly probably resides in the atomic structure of the surface in the different faces of the LaB_6 crystals.[102,103,106,112] According to current views, the (100) surface consists of a plane of La ions, whereas in the (110) and (111) faces the La ions are displaced from their equilibrium positions by ~1.66 and 1.2 Å respectively (Fig.7), i.e. the greater the displacement of the La ions "from within" towards the surface, the lower is the work function. According to some workers[100–103] the difference in work function of the LaB_6 faces is explained by differences in the electrical dipole moments created by the positively charged La^{3+} ions and the octahedra of B atoms in the surface layer: the work function of the (100) and (110) faces is lower than that of the (111) face because their dipole moment is higher.

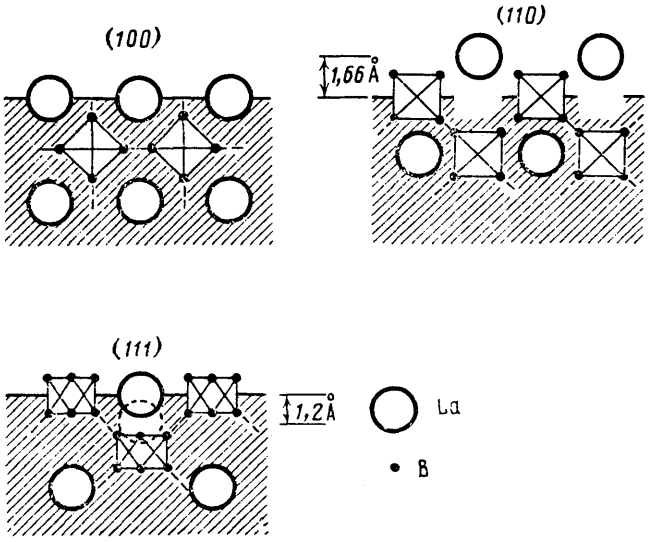


Figure 7. Surface structure of different faces of the LaB_6 crystal (from Ref.103).

Recent studies[104–106] of the energy structure of the LaB_6 surface have identified several peaks in the region of 1.5 to 3 eV below the Fermi level from the UPS spectra of the (100), (110), and (111) faces. These peaks are attributed to the so-called "dangling" bonds, i.e. to uncompensated bonds of the surface boron atoms.[107] The peaks disappear when oxygen is adsorbed on the LaB_6 surface, indicating an interaction between the oxygen atoms and the uncompensated boron bonds.[96] Adsorbed oxygen (or other gases) can form a dipolar surface layer which alters the surface potential and therefore also the work function.[94–96]

However, residual gases, including oxygen, can increase the emission rather than impair the emission properties.[108,109] Thus, it was found[109] that at an oxygen partial pressure of 10^{-10}–$(1-3) \times 10^{-9}$ mmHg the work function of the (210) face is ~0.2 eV lower than for the clean surface, and the emission is correspondingly higher. No explanation has yet been suggested.

Problems of adsorption on the surface of LaB_6 monocrystals are of practical as well as of theoretical interest in relation to the controlled modification of the emission characteristics by the simultaneous adsorption of several elements. For example, it has been shown[110] that the adsorption of Cs on the clean (100) and (110) faces of a LaB_6 crystal lowers the work function from 2.78 to 1.97 and 1.88 eV respectively. However, if the Cs is adsorbed on the same surfaces previously covered with oxygen the work function falls to 1.35 and 1.47 eV respectively. These surface coatings were found to have a reasonable thermal stability: thus, the Cs is desorbed from a clean

(100) surface of the LaB_6 crystal at ~900 K, whereas on a surface previously coated with oxygen desorption takes place at ~1150 K.[111] The work function of the clean (100) face may not be the lowest, of course. Higher-index faces have also given low values of the work function: $\phi_R = 2.3$ eV for the (321) face,[85] $\phi_{ef} = 2.41$ eV for (364),[84] $\phi = 2.2$ eV [112,113] and $\phi_R = 2.48$ eV for (210).[102]

Another method of improving the emission properties of LaB_6 monocrystals relies on doping the material. We know that the work function is given by the expression

$$\varphi = \chi - \mu \qquad (2)$$

where χ is the difference between the electrical potentials in the bulk of the metal and in the vacuum near the surface, and μ is the chemical potential of the electron gas in the metal ($\mu \approx E_F$, where E_F is the Fermi energy).[82] By varying χ or μ (for example, by doping) we can vary the work function of the LaB_6 in the required direction. In this respect the most promising materials are solid solutions based on LaB_6 in which some of the La atoms are replaced by other materials, especially rare-earth and alkaline-earth metals.

The emission properties of some solid solutions have been measured both on monocrystals and on polycrystalline samples.[51,52,88] It was found that the work function of the (100) face of the solid solution is higher than that of the LaB_6 crystals, and relatively insensitive to the nature of the added metal. It was also shown[52] that the surface of crystals of the LaB_6 solid solutions gradually become enriched in La (with respect to the bulk) at high temperatures as a result of the preferential evaporation of the second metallic component. These materials show a characteristic instability of the emission current.[88] Similar phenomena have been observed in polycrystalline solid solutions of the MB_6 type, where M = La, Y, Sc.[114] Nevertheless further work on these materials should be of interest.

Studies of field emission from LaB_6 monocrystals are also of great theoretical and practical interest in connection with the development of new materials for auto-emission cathodes.[115-117]

The first studies of field emission in an ion beam were carried out with monocrystals prepared by liquid-phase[115,118] and by solution methods.[119] It was shown that the image of a LaB_6 point in He ions at 78 K has an irregular structure. The quality of the image was worse than for metal points. However, later workers obtained images of LaB_6 points with a regular structure.

Studies of the effect of various gases (hydrogen,[120] neon, oxygen, and hydrogen[121]) on the image from a LaB_6 point revealed a rearrangement in a hydrogen atmosphere from low-index faces into faces with higher indices of the type of {012}, {013}, {112}, etc., whereas in the presence of oxygen the surface becomes strongly disordered, with cluster formation. The hydrogen reacts primarily with the surface B atoms,[120] and the oxygen with both the La and the B atoms.[121]

A study[122] of the mechanism of formation of images from points of LaB_6 and $La_{0.58}Sm_{0.42}B_6$ monocrystals in helium, neon, and hydrogen ions showed that only the metal ions (La or La and Sm) contribute to the formation of the image. However, others[121] assume that the main contribution to the formation of images of the points in He and Ne is from the uncompensated bonds of the boron atoms in the octahedra. This point of view is confirmed to some extent by studies of LaB_6 by the atomic probe method, with mass spectrometric analysis of the ions produced by field evaporation.[123,124]

Swanson[84] measured the work function and the field emission current of monocrystal points, and he concluded that LaB_6 has no real advantage as a field emitter over other refractory compounds. However, by generating microscopic projections on a point from a <100> LaB_6 monocrystal an emission current of ~10^{-5} A was obtained from the projection,[125] corresponding to a source brightness of ~10^{11} A cm^{-2} steradian^{-1}.

Nevertheless further studies of LaB_6 in an ion beam are of interest both from the standpoint of a more detailed understanding of the surface structure at the atomic level and to explain the mechanism of image formation from points of compounds. Furthermore it has been shown[102] that the evaporation under the influence of a field and the reconstruction of a surface can affect the concentration of La atoms, and therefore also the work function of the various faces. This work is extremely relevant, because using a thermo-emission cathode made of monocrystalline LaB_6 in an electron gun produces a spotty emission,[126,127] which can be eliminated (while at the same time increasing the brightness of the image) by operating the cathode in the thermal-field emission mode.[109]

5. Some Practical Applications

Because of the unique combination of physicochemical properties offered by LaB_6 its practical applications are extremely varied, and we shall only dwell on the most interesting and important results (in our opinion). The use of LaB_6 as a thermo-electronic emitter in the cathodes assemblies of various types of device should be mentioned first. The advantages of cathodes made of sintered LaB_6 over tungsten cathodes for use in scanning electron microscopes have long been recognised.[128-130]

The preparation of LaB_6 monocrystals stimulated the production of monocrystalline thermo-emission cathodes, the study of their characteristics, and the search for possible alternatives to oxide and tungsten cathodes.[88,106,118,126,131-143] The operating characteristics of a monocrystalline LaB_6 cathode used in commercial equipment (microanalysers and Auger spectrometers) in place of a tungsten cathode have been measured.[106,133,134] The LaB_6 cathode is shown to be brighter than the tungstem cathode (2×10^5 A cm^{-2} steradian^{-1} and 1.5×10^4 A cm^{-2} steradian^{-1} respectively), and to have a more stable emission current (better than 1×10^{-3} A h^{-1}). It was also shown[134] that a cathode consisting of a LaB_6 point with a <100> orientation can produce a cathode current density of ~50 A cm^{-2}, combined with an operating life of more than 300 h. An electron gun with a cathode made from a zone melted LaB_6 single crystal cut in the <100> direction has been developed,[135] giving an optimum brightness of 2.5×10^5 A cm^{-2} steradian^{-1} at a cathodic current density of 50 A cm^{-2}. A cathode with a monocrystal oriented in the <100> direction was reported[84] to give a current density of ~10 A cm^{-2} at 1600 to 1700 K; under these conditions the rate of evaporation of the cathode was ~1 μm year^{-1}.

The successful replacement of a rhenium cathode by a monocrystalline LaB_6 cathode in a commercial mass spectrometer has been claimed.[136] The life of the LaB_6 cathode is 10 times greater than that of the rhenium cathode, and its working temperature is lower (1750 K instead of 2500 K), which allows thermally unstable compounds to be analysed. The replacement[139] of a tungsten cathode in a micro-focus X-ray source by a LaB_6 monocrystal has given a 20 times higher current density at the target with an operational life of ~800 h.

A monocrystalline LaB_6 cathode has been fitted[140] to an electron microscope, giving a brightness of 2×10^6 A cm^{-2} steradian^{-1} and a stable operation time of over 100 h; the resolution of the microscope was 0.14 nm.

Another promising application of monocrystalline LaB_6 cathodes is in the production of integrated circuits by electron-beam lithography.[138] A very precise and fast lithographic

system has been based[141] on a monocrystalline LaB_6 cathode consisting of a flattened point, giving an electron beam 6.4 × 6.4 μm in cross-section and a current density of 10A cm^{-2}.

Work is also in progress on improved designs of cathode assemblies[142] and on optimised conditions for using the monocrystalline LaB_6 cathodes.[143] Thus a new method of attaching the monocrystal of lanthanum hexaboride to the cathode assembly gives a working life of 1000 h at a cathode working temperature of 1800 K.[142]

Considerable effort is devoted also to the use of polycrystalline LaB_6. For example, it has been shown that cathodes made from hot-pressed or sintered polycrystalline LaB_6 are potentially useful for high-current ion sources in atomic technology,[144-147] especially for the production of a high-density plasma in apparatus of the "Tokamak" type.[145,146] Sintered LaB_6–ZrB_6 compositions have also been studied with the aim of improving the mechanical and emission properties of LaB_6 cathodes.[148]

Powdered LaB_6 has been used in the isotopic analysis of iodine,[149] and found to give a relative sensitivity better than materials like the W–Th alloy, ZrC, Hf, and Re.

A study of the catalytic activity of the clean surface of LaB_6 powders towards the hydrogen–deuterium isotope exchange has been reported.[150] At 159 K the specific activity of LaB_6 is two orders of magnitude greater than the activity of γ-Al_2O_3, and only slightly lower than the activity of Pt or Ni.

---o0o---

Thus the preparation of perfect monocrystals of LaB_6 by any of the methods examined requires accurate information on the La–B phase diagram, and in particular on the homogeneity region of LaB_6. Another important requirement is a very accurate characterisation of the resulting LaB_6 crystals in both composition and structure, to allow these data to be related to the other properties of the material. Only by establishing these relationships can the controlled production of perfect and defect-free LaB_6 monocrystals, by any method, be achieved.

REFERENCES

1. M.M.Korsukova and V.N.Gurin, in "Current Topics in Materials Science", v.11 (E.Kaldis, Editor), Amsterdam–New York–Oxford–Tokyo, 1984, p.389.
2. L.Andrieux, Ann.Chim., 1929, **12**, 423.
3. K.Johnson and A.N.Daane, J.Phys.Chem., 1961, **65**, 909.
4. K.E.Spear, in "Boron and Refractory Borides" (V.I.Matkovich, Editor), Springer, Berlin–Heidelberg–New York, 1977, p.439.
5. E.Storms and B.Mueller, J.Phys.Chem., 1978, **82**, 51.
6. M.J.McKelvy, L.Eyring, and E.K.Storms, J.Phys. Chem., 1984, **88**, 1785.
7. K.Kato, I.Kawada, C.Oshima, and Sh.Kawai, Acta. Cryst., B, 1974, **30**, 2933.
8. M.von Stackelberg and S.Weinbaum, Z.phys.Chem., 1932, **19**, 314.
9. L.Pauling and S.Weinbaum, Z.Krist., 1934, **87**, 181.
10. G.V.Samsonov, "Tugoplavkie Soedineniya Redkozemel'nykh Metallov" (Refractory Compounds of the Rare-earth Metals), Izd.Metallurgiya, Moscow, 1964.
11. G.V.Samsonov, Yu.B.Paderno, and S.U.Kreingol'ts, Zhur.Prikl.Khim., 1961(1), 10.
12. N.N.Zhuravlev, R.M.Manelis, N.V.Gramm, and A.A.Stepanova, Poroshkovaya Metallurgiya, 1967(2), 95.
13. F.G.Mamedov, G.A.Meerson, N.N.Zhuravlev, and Ya.S.Umanskii, Izv.Akad.Nauk SSSR, Neorg.Materialy, 1967, **3**, 950.
14. G.A.Meerson and F.G.Mamedov, Izv.Akad.Nauk SSSR, Neorg.Materialy, 1967, **3**, 802.
15. N.N.Zhuravlev, I.A.Belousova, R.N.Manelis, and N.A.Belousova, Kristallografiya, 1970, **15**, 836.
16. M.I.Aivazov, V.A.Bashilov, K.A.Zinchenko, and R.R.Kagramanova, Poroshkovaya Metallurgiya, 1979(1), 46.
17. M.M.Korsukova, T.Lundström, L.-E.Tergenius, and V.N.Gurin, "Tezisy Dokladov Chetvertoi Vsesoyuznoi Konferentsii po Kristallokhimii Intermetallicheskikh Soedinenii" (Abstracts of Papers Presented to the Fourth All-Union Conference on the Crystal Chemistry of Intermetallic Compounds), Izd.L'vov.Univ., 1983, p.108.
18. Yu.B.Paderno and T.Lundström, Acta Chem.Scand., A, 1983, **37**, 609.
19. N.N.Zhuravlev, R.M.Manelis, I.A.Belousova, and V.Kh.Nurmukhamedov, Izv.Akad.Nauk SSSR, Neorg. Materialy, 1973, **9**, 1162.
20. S.P.Gordienko, V.V.Fenochka, and G.I.Veksman, "Termodinamicheskie Svoistva Lantanoidov" (Thermodynamic Properties of the Lanthanides), Izd.Naukova Dumka, Kiev, 1979.
21. P.V.Hafner, Thesis, Zürich, 1976.
22. V.I.Gurin, Izv.Akad.Nauk SSSR, Neorg.Materialy, 1973, **9**, 1289.
23. H.Klotz, Naturwiss, 1965, **52**, 451.
24. E.I.Givargizov and L.N.Obolenskaya, J.Crystal Growth, 1981, **51**, 190.
25. T.Niemysky and E.Kierzec-Pecold, J.Cryst.Growth, 1968, **3/4**, 162.
26. S.Motojima, I.Takahashi, K.Sugijama, J.Cryst. Growth, 1978, **44**, 106.
27. T.Tanaka, E.Bannai, S.Kawai, and T.Yamane, J.Cryst.Growth, 1975, **30**, 193.
28. K.Takagi and M.Ishii, J.Cryst.Growth, 1977, **40**, 1.
29. J.D.Verhoeven, E.D.Gibson, M.A.Noack, and R.J.Conzemius, J.Cryst.Growth, 1976, **36**, 115.
30. M.A.Noack and J.D.Verhoeven, J.Cryst.Growth, 1980, **49**, 595.
31. V.V.Morozov, V.Ya.Shlyuko, A.I.Goncharuk, and P.I.Loboda, Elektronnaya Tekhnika, Materialy, 1982(2), 15.
32. Yu.B.Paderno, V.I.Lazorenko, and A.V.Kovalev, Poroshkovaya Metallurgiya, 1981(10), 60.
33. Yu.B.Paderno, V.I.Lazorenko, N.I.Buryak, A.V.-Kovalev, A.A.Matvienko, and A.P.Galasun, Poroshkovaya Metallurgiya, 1983(1), 56.
34. Z.Fisk, A.S.Cooper, P.H.Schmidt, and R.N.Castellano, Mater.Res.Bull., 1972, **7**, 285.
35. A.I.Arko, G.Crabtree, D.Karim, F.Mueller, L.R.Windmiller, J.B.Ketterson, and Z.Fisk, Phys. Rev., B 1976, **13**, 5240
36. L.W.Swanson and T.Dickinson, Appl.Phys.Letters, 1976, **28**, 578.
37. P.H.Schmidt, D.C.Joy, L.D.Longinotti, H.J.Leamy, S.D.Ferris, and Z.Fisk, Appl.Phys.Letters, 1976, **29**, 400.
38. M.Futamoto, T.Aita, and U.Kawabe, Jap.J.Appl. Phys., 1975, **14**, 1263.

39. T.Aita, U.Kawabe, and Y.Honda, Jap.J.Appl.Phys., 1974, **13**, 391.
40. M.M.Korsukova, Thesis, L'vov, 1977.
41. N.N.Stepanov, A.Yu.Zyuzin, S.G.Shul'man, V.N. Gurin, M.M.Korsukova, S.F.Nikanorov, and I.A.Smirnov, Fiz.Tverdogo Tela, 1978, **20**, 935.
42. V.N.Gurin, M.M.Korsukova, S.P.Nikanorov, I.A.Smirnov, N.N.Stepanov, and S.G.Shul'man, J.Less-common Metals, 1979, **67**, 115.
43. M.M.Korsukova, A.V.Nardov, and V.N.Gurin, "Rashirennye Tezisy Dokladov Shestoi Mezhdunarodnoi Konferentsii po Rostu Kristallov" (Extended Abstracts of the Papers Presented to the Sixth International Conference on Crystal Growth), Moscow, 1980, **3**, 259.
44. C.H.Olsen and A.V.Cafiero, J.Crystal Growth, 1978, **44**, 287.
45. I.V.Zubeck, R.S.Feigelson, R.A.Huggins, and P.A.Pettit, J.Crystal Growth, 1976, **34**, 85.
46. N.F.Chaban and Yu.B.Kuz'ma, Izv.Akad.Nauk UkrSSR, 1971, p.1043.
47. V.N.Gurin and M.M.Korsukova, Progress in Crystal Growth and Characterisation, 1983, **6**, 59.
48. G.H.Olsen and A.V.Cafiero, US P.4260525(1981).
49. T.B.Zhukova, M.M.Korsukova, V.N.Gurin, and A.V.Nardov, Izv.Akad.Nauk SSSR, Neorg.Materialy, 1981, **17**, 161.
50. K.-T.Vil'ke, "Vyrashchivanie Kristallov" (Crystal Growth), Izd.Nedra, Moscow, 1977, p.249.
51. P.H.Schmidt and D.C.Joy, J.Vacuum Sci.Technol., 1978, **15**, 1809.
52. M.Futamoto, M.Nakazawa, and U.Kawabe, Surface Sci., 1980, **100**, 470.
53. P.I.Antonov and S.P.Nikanorov, in "Shaped Crystal Growth" (G.W.Gullen, T.Shurek, and P.I.Antonov, Editors), North Holland, Amsterdam, 1980, p.3.
54. M.M.Korsukova, T.Lundström, V.N.Gurin, and L.-E.Tergenius, Z.Kristallogr., 1984, **168**, 299.
55. M.M.Korsukova, T.Lundström, V.N.Gurin, and L.-E.Tergenius, J.Less-common Metals, 1986, **117**, 73.
56. M.Ishii, T.Tanaka, E.Bannai, and Sh.Kawai, J.Phys. Soc.Japan, 1976, **41**, 1071.
57. T.Tanaka, J.Yoshimoto, M.Ishii, E.Bannai, and Sh.Kawai, Solid State Comm., 1977, **22**, 203.
58. T.Tanaka, T.Akahane, E.Bannai, Sh.Kawai, N.Tsuda, and Y.Ishizawa, J.Phys., C, 1976, **9**, 1235.
59. Yu.B.Paderno, E.S.Garf, T.Nemyskii, and I.Pratska, Poroshkovaya Metallurgiya, 1969(10), 55.
60. H.C.Longuet-Higgins and M.de V.Roberts, Proc. Roy Soc., 1954, **224**, 336.
61. M.Jamazaki, J.Phys.Soc.Japan, 1957, **12**, 1.
62. C.Kittel, "Introduction to Solid State Physics" (Translated into Russian), Izd.Nauka, Moscow, 1978.
63. J.Ishizawa, T.Tanaka, E.Bannai, and Sh.Kawai, J.Phys.Soc.Japan, 1977, **42**, 112.
64. I.Frankowski and P.Wachter, Solid State Comm., 1982, **41**, 577.
65. A.P.I.van Deursen, Z.Fisk, and A.R.deVroomen, Solid State Comm., 1982, **44**, 609.
66. P.F.Walch, D.E.Ellis, and F.M.Mueller, Phys.Rev., B, 1977, **15**, 1859.
67. A.Hasegawa and A.Yanase, J.Phys.F, 1977, **7**, 1245.
68. A.Hasegawa and A.Yanase, J.Magnetism and Magnetic Mater., 1980, **15/18**, Pt.2, 887.
69. M.Aono, T.C.Chiang, J.A.Knapp, T.Tanaka, and E.Eastman, Solid State Comm., 1979, **32**, 271.
70. E.Kierzeck-Pecold, Physica Status Solidi, 1969, **33**, 523.
71. L.A.Ivanenko, Yu.B.Paderno, and A.N.Pilyankevich, Poroshkovaya Metallurgiya, 1978(8), 38.
72. V.I.Bessaraba, L.A.Ivanchenko, and Yu.B.Paderno, J.Less-common Metals, 1979, **67**, 505.
73. L.A.Ivanchenko, Yu.B.Paderno, A.N.Pilyankevich, V.L.Bekenev, V.V.Koval'chuk, A.F.Onipko, I.N.Perepelitsa, V.V.Sichkar', and L.I.Cherenko, Izv.Akad.Nauk SSSR, Neorg.Materialy, 1980, **16**, 1551.
74. V.I.Bessaraba, T.I.Makarenko, and Yu.B.Paderno, Zhur.Prikl.Spektrosk., 1980, **33**, 527.
75. V.N.Gurin, M.M.Korsukova, M.G.Karin, K.K.Sidorin, I.A.Smirnov, and A.I.Shelykh, Fiz.Tverdogo Tela, 1980, **22**, 715.
76. A.I.Shelykh, K.K.Sidorin, M.G.Karin, V.N.Bobrikov, M.M.Korsukova, V.N.Gurin, and I.A.Smirnov, J.Less-common Metals, 1981, **82**, 291.
77. I.Mörke, V.Dvorak, and P.Wachter, Solid State Comm., 1981, **40**, 331.
78. V.N.Paderno, Yu.B.Paderno, A.N.Pilyankevich, V.I.Lazorenko, and S.I.Bulychev, J.Less-common Metals, 1979, **67**, 431.
79. G.V.Samsonov and I.M.Vinitskii, "Tugoplavkie Soedineniya" (Refractory Compounds), Izd.Metallurgiya, Moscow, 1976.
80. V.V.Morozov, B.I.Mal'tsev, S.N.Dub, P.I.Loboda, and V.S.Kresanov, Izv.Akad.Nauk SSSR, Neorg. Materialy, 1984, **20**, 421.
81. M.Futamoto, T.Aita, and U.Kawabe, Materials Res. Bull., 1979, **14**, 1329.
82. L.N.Dobretsov and M.V.Gomoyunova, "Emissionnaya Elektronika" (Emission Eletronics), Izd.Nauka, Moscow, 1966, p.117.
83. E.K.Storms and B.A.Mueller, J.Appl.Phys., 1979, **50**, 3691.
84. L.W.Swanson, M.A.Gesley, and P.R.Davis, Surface Sci., 1981, **107**, 263.
85. H.Jamauchi, K.Takagi, I.Unito, and U.Kawabe, Appl. Phys.Letters, 1976, **29**, 638.
86. C.Oshima, E.Bannai, T.Tanaka, and Sh.Kawai, J.Appl.Phys., 1977, **48**, 3925.
87. A.Berrada, J.Mercurio, J.Etourneau, and P.Hagenmüller, J.Less-common Metals, 1978, **59**, 7.
88. P.H.Schmidt, L.D.Longinotti, D.C.Joy, S.D.Ferris, H.J.Leamy, and Z.Fisk, J.Vacuum Sci.Technol., 1978, **15**, 1554.
89. L.W.Swanson and D.McNeely, Surface Sci., 1979, **83**, 11.
90. M.Futamoto, M.Nakazawa, K.Usami, S.Noshoki, and U.Kawabe, J.Appl.Phys., 1980, **51**, 3869.
91. C.Oshima, E.Bannai, T.Tanaka, and Sh.Kawai, Jap. J.Appl.Phys., 1977, **16**, 965.
92. E.Goldstein and D.I.Szostak, Surface Sci., 1978, **74**, 461.
93. M.Aono, T.Tanaka, E.Bannai, and Sh.Kawai, Appl. Phys.Letters, 1977, **31**, 323.
94. R.Nishitani, Sh.Kawai, H.Iwasaki, S.Nakamura, M.Aono, and T.Tanaka, Surface Sci., 1980, **92**, 191.
95. S.A.Chambers and L.W.Swanson, Surface Sci., 1983, **131**, 385.
96. R.Nishitani, C.Oshima, M.Aono, T.Tanaka, S.Kawai, H.Iwasaki, and S.Nakamura, Surface Sci., 1982, **115**, 48.
97. N.Nakazawa, M.Futamoto, S.Hosoki, and K.Usami, Jap.J.Appl.Phys., 1980, **19**, 1267.
98. S.Klauser and E.Bas, Appl.Surface Sci., 1979, **3**, 356.
99. M.Aono, C.Oshima, T.Tanaka, E.Bannai, and Sh.Kawai, J.Appl.Phys., 1978, **49**, 2761.

100. R.Nishitani, M.Aono, T.Tanaka, C.Oshima, Sh.Kawai, H.Iwasaki, and S.Nakamura, Surface Sci., 1980, **93**, 535.
101. M.Aono, R.Nishitani, C.Oshima, T.Tanaka, E.Bannai, and S.Kawai, J.Appl.Phys., 1979, **50**, 4802.
102. M.A.Gesley, P.R.Davis, and L.W.Swanson, "Proceedings of the Twenty-ninth International Field Emission Symposium" (H.-O.Andrén and H.Nordén, Editors), Almqvist and Wiksell, Stockholm, 1982, p.121.
103. R.E.Watson and M.L.Perlman, Surface Sci., 1982, **122**, 371.
104. M.Aono, T.Tanaka, E.Bannai, C.Oshima, and Sh.Kawai, Phys.Rev., B, 1977, **16**, 3489.
105. R.Nishitani, M.Aono, T.Tanaka, Sh.Kawai, H.Iwagaki, C.Oshima, and S.Nakamura, Surface Sci., 1980, **95**, 341.
106. Sh.Kawai, Mem.Inst.Sci.Ind.Res.Osaka Univ., 1983, **40**, 47.
107. M.Tomasek and S.Pick, Czech.J.Phys., 1979, **29**, 557.
108. R.Shimizu, H.Onoda, H.Hagiwara, and S.Ishii, J.Appl.Phys., 1981, **52**, 6316.
109. R.Shimizu, H.Onoda, J.Hashimoto, and H.Hagiwara, J.Appl.Phys., 1984, **55**, 1379.
110. S.A.Chambers, F.R.Davis, L.W.Swanson, and M.A.Geesly, Surface Sci., 1982, **118**, 75.
111. S.A.Chambers, F.R.Davis, L.W.Swanson, and M.A.Geesly, Surface Sci., 1982, **118**, 93.
112. C.Oshima, M.Aono, T.Tanaka, R.Nishitani, and Sh.Kawai, J.Appl.Phys., 1980, **51**, 997.
113. C.Oshima, M.Aono, T.Tanaka, Sh.Kawai, R.Shimizu, and H.Hagawara, J.Appl.Phys., 1980, **51**, 1201.
114. A.I.Kondrashev, N.I.Siman, and I.A.Podchernyaeva, Poroshkovaya Metallurgiya, 1977(8), 62.
115. E.Windsor, Proc.Inst.Elec.Engineers, 1969, **116**, 348.
116. M.I.Elinson and G.A.Kudintseva, Radiotekh.i Elektronika, 1962, **7**, 1151.
117. G.A.Kudintseva, G.M.Kudintseva, B.P.Savchenko, and V.N.Shrednik, Izv.Akad.Nauk SSSR, Neorg. Materialy, 1971, **35**, 239.
118. R.Shimizu, Y.Kataoka, T.Tanaka, and Sh.Kawai, Jap.J.Appl.Phys., 1975, **14**, 1089.
119. M.Futamoto, S.Hosoki, H.Okano, and U.Kawabe, J.Appl.Phys., 1977, **48**, 3541.
120. S.Nakamura, Y.S.Ng, T.Tsong, and S.B.McLane, Surface Sci., 1979, **87**, 656.
121. Q.Chen, T.Adachi, and S.Nakamura, "Extended Abstracts of the Papers Presented to the Twenty-seventh International Field Emission Symposium", Tokyo, 1980, p.377.
122. M.Futamoto and U.Kawabe, Surface Sci., 1980, **93**, L117.
123. K.Murakami, T.Adachi, O.Komoda, T.Kuroda, and S.Nakamura, "Proceedings of the Twenty-ninth International Field Emission Symposium" (H.-O.Andrén and H.Nordén, Editors), Almqvist and Wiksell, Stockholm, 1982, p.257.
124. K.Murakami, T.Adachi, T.Kuroda, S.Nakamura, and O.Komoda, Surface Sci., 1983, **124**, L25.
125. T.Innoue, M.Nakada, T.Uozomi, and E.Sugata, J.Vacuum Sci.Technol., 1982, **21**, 952.
126. Y.Furukawa, M.Yamabe, A.Itoh, and T.Inagaki, J.Vacuum Sci.Technol., 1982, **20**, 199.
127. T.Takigawa, S.Yoshi, I.Sasaki, K.Motoyama, and T.Meguro, Jap.J.Appl.Phys., 1980, **19**, L537.
128. A.N.Broers, J.Appl.Phys., 1967, **38**, 1991.
129. A.N.Broers, J.Phys.E, Ser.2, 1969, **2**, 273.
130. S.F.Vogel, Rev.Sci.Instr., 1970, **41**, 585.
131. D.E.Gibson and J.D.Verhoeven, J.Phys.E., 1975, **8**, 1003.
132. J.D.Verhoeven and D.E.Gibson, J.Phys.E., 1976, **9**, 65.
133. R.Shimizu, T.Shinike, Sh.Kawai, and T.Tanaka, Jap.J.Appl.Phys., 1977, **16**, 669.
134. R.Shimizu, T.Shinike, S.Ishimura, Sh.Kawai, and T.Tanaka, J.Vacuum Sci.Technol., 1978, **15**, 922.
135. N.Nakasuji and H.Wada, J.Vacuum Sci.Technol., 1980, **17**, 1367.
136. L.Kelner, H.M.Fales, S.P.Markey, and C.K.Crawford, Internat.J.Mass Spectrom.Ion Phys., 1982, **43**, 249.
137. M.Yamabe, Y.Furukawa, and T.Inagaki, J.Vacuum Sci.Technol.A, 1984, **2**, 1361.
138. M.B.Heritage, J.Vacuum Sci.Technol.A, 1975, **12**, 1135.
139. S.Aoki and Y.Sakayanagi, Jap.J.Appl.Phys., 1981, **20**, 2419.
140. N.M.Moiseeva, I.F.Anaskin, and P.A.Stoyanov, "Tezisy Dokladov Dvenadtsatoi Vsesoyuznoi Konferentsii po Elektronnoi Mikroskopii" (Abstracts of the Papers Presented to the Twelfth All-Union Electron Microscopy Conference), Izd.Nauka, Moscow, 1982, p.36.
141. N.Saitou, M.Okumura, G.Matsuoka, T.Matsuzaka, T.Komoda, and Y.Sakitani, J.Vacuum Sci.Technol. B, 1985, **3**, 98.
142. P.R.Davis, G.A.Schwind, and L.W.Swanson, J.Vacuum Sci.Technol.B, 1986(4), 112.
143. P.R.Davis, L.W.Swanson, J.J.Hutta, and D.L.Jones, J.Materials Sci., 1986, **21**, 825.
144. V.Ya.Shlyuko, N.N.Semashko, N.P.Malakhov, V.V.Morozov, V.S.Kresanov, and V.L.Valentinov, in "Voprosy Atomnoi Nauki i Tekhniki. Seriya Termoyadernyi Sintez" (Problems in Atomic Science and Technology. Thermonuclear Synthesis Series), No.2–4. Izd.Inst.Atomnoi Energii, Moscow, 1979, p.107.
145. V.Ya.Shlyuko, N.N.Semashko, N.P.Malakhov, V.S.Kresanov, V.V.Morozov, and Yu.I.Grusha, in "Voprosy Atomnoi Nauki i Tekhniki. Seriya Termoyadernyi Sintez" (Problems in Atomic Science and Technology. Thermonuclear Synthesis Series). No.1–9, Izd.Inst.Atomnoi Energii, Moscow, 1982, p.83.
146. D.M.Goebel, J.T.Crow, and A.T.Forrester, Rev.Sci. Instr., 1978, **49**, 469.
147. T.Shintake, K.Ohba, M.Matoba, and A.Katase, Jap. J.Appl.Phys., 1981, **20**, 341.
148. S.S.Ordan'yan, Yu.B.Paderno, I.K.Khoroshilova, E.E.Nikolaeva, and E.V.Maksimova, Poroshkovaya Metallurgiya, 1983(11), 87.
149. J.E.Delamore, Internat.J.Mass Spectrom.Ion Phys., 1982, **43**, 273.
150. T.Nagaki, Y.Inoue, I.Kojima, and I.Yasumori, J.Phys.Chem., 1980, **84**, 1919.

Ioffe Physico-technical Institute
of the USSR Academy of
Sciences, Leningrad